 https://doi.org/10.3311/PPci.16389

Periodica Polytechnica Civil Engineering, 64(3), pp. 828–844, 2020

Comparing H_2 and H_∞ Algorithms for Optimum Design of Tuned Mass Dampers under Near-Fault and Far-Fault Earthquake Motions

Ali Kaveh[1*], Mazyar Fahimi Farzam[2], Rasool Maroofiazar[3]

[1] School of Civil Engineering, Iranian University of Science and Technology, Tehran, P.O. Box 16846–13114, Iran
[2] Department of Structural Engineering, University of Maragheh, Maragheh, P.O. Box: 83111–55181, Iran
[3] Department of Mechanical Engineering, University of Maragheh, Maragheh, P.O. Box: 83111–55181, Iran
[*] Corresponding author, e-mail: alikaveh@iust.ac.ir

Received: 05 May 2020, Accepted: 12 May 2020, Published online: 11 June 2020

Abstract

In this study, the robust optimum design of Tuned Mass Damper (TMD) is established. The H_2 and H_∞ norm of roof displacement transfer function are implemented and compared as the objective functions under Near-Fault (NF) and Far-Fault (FF) earthquake motions. Additionally, the consequences of different characteristics of NF ground motions such as forward-directivity and fling-step are investigated on the behavior of a benchmark 10-story controlled structure. The Colliding Bodies Optimization (CBO) is employed as an optimization technique to calculate the optimum parameters of the TMDs. The resulting statistical assessment shows that the H_∞ objective function is rather superior to H_2 objective function for optimum design of TMDs under NF and FF earthquake excitations. Finally, the robustness of the designed TMDs is evaluated under a large set of natural ground motions.

Keywords

Tuned Mass Dampers, Near-Fault earthquake motions, robust design, optimum design, metaheuristic algorithm CBO

1 Introduction

Passive TMDs are one of the well-established and most studied devices used in vibration control of the real buildings and structures due to their simplicity, reliability, and effectiveness. Elias and Matsagar [1] presented a detailed updated state-of-the-art review on the performance of these absorbers theoretically and experimentally applied in structures. Their review illustrates many different aspects of the TMD, especially the response control of structures under winds and earthquakes that are investigated by many researchers and covers the theoretical backgrounds of this control device. A broad list of TMDs controlled structures are accessible by Gutierrez Soto and Adeli [2], and one of the notable recent real application is a new eddy-current TMD, the heaviest one (about 1000-ton) ever designed, at the roof of the second tallest building in the world (the 125-story Shanghai Center Tower in Shanghai). In this building, innovatively, unique protective mechanisms have been adopted to prevent excessively large amplitude of the TMD under extreme wind or earthquake loading scenarios (Lu et al. [3]).

Sun et al. [4] reviewed the history of the TMDs probably first introduced by Frahm in 1911 for reducing the rocking motion of ships. It is normally preferred the TMD parameters to be optimized to enhance its controllability. For the optimum tuning of TMDs, several approaches have been proposed in the literature. Conventional mathematical methods that need substantial gradient information and numerical iteration techniques are two main categories of these approaches (Elias and Matsagar [1]).

Recently, due to the complexity of tuning problems involved in MDOF structures with inherent damping under earthquake excitations, other numerical optimization techniques have been applied to acquire the best performance for TMDs.

Although under narrow-band dynamic loads (wind, sea wave, pedestrians) and long duration ground motions i.e., FF earthquakes, the TMDs performance are ascertained by many researchers, their seismic performance is controversially subjected to pulse-like motions such as NF earthquakes, and they may not have enough time to produce significant control force (Lin et al. [5], Matta [6]).

Cite this article as: Kaveh, A., Farzam, M. F., Maroofiazar, R. "Comparing H_2 and H_∞ Algorithms for Optimum Design of Tuned Mass Dampers under Near-Fault and Far-Fault Earthquake Motions", Periodica Polytechnica Civil Engineering, 64(3), pp. 828–844, 2020. https://doi.org/10.3311/PPci.16389

NF ground motions may expose structures to high-input energy at the beginning of the record with short-duration impulsive motions. Since TMD cannot immediately start to dissipate the vibration energy, Lin et al. [5] applied an initial velocity to the TMD opposite to the direction of structural impulsive motion to accelerate its motion and to increase TMD performance under NF earthquake excitations. Results show that an optimum TMD initial velocity can be applied; however, due to the limitation of moving space for TMD, using an optimum velocity may be impractical. Matta [6] introduced a new optimization method as an alternative to the classical H_∞ approach and calculated optimum values of the TMD parameters to reduce the structural response under a large set of NF records possessing pulse-like characteristics. The results of this study indicate that either the optimum frequency ratio or the optimum damping ratio should be significantly lower than the optimum values determined for harmonic loads. Domizio et al. [7] studied the application of TMD for improving the structural safety of existing buildings subjected to a series of NF seismic records. In this context, the TMD performance located on an MDOF structure is analyzed. In particular, the ability to prevent the collapse by the implementation of this device is investigated, and for each record, the minimum value of peak ground acceleration that leads to the structural collapse is obtained. They concluded that when the dominant frequency of the excitation is close to the fundamental frequency of the structure, the absorber is effective in decreasing the probability of structural collapse.

Within a wide on-going research Salvi et al. [8] optimized an innovative scenario of hybrid TMD composed of a passive TMD and a feedback closed-loop active controller added on the top of an SDOF and a 10-story shear-type frame building under impulse excitation to control the average and peak structural response. In a recent study, Salvi et al. [9] also considered a linear damped SDOF and a linear TMD added on it subjected to pulse-like base displacement excitations and extracted the optimum condition toward best TMD calibration focused on an average response index.

Although a few previous papers have studied the performance of TMD controlled buildings under NF and FF ground motions, a thorough probabilistic assessment using NF ground motions with fling-step and forward-directivity features has not been conducted yet. Hence, in current work, the possible advantages of the H_2, H_∞ and other tuning methods for optimum design of TMD is evaluated for a 10-story controlled shear building, under FF and NF ground motions with fling-step or forward-directivity characteristics.

The rest of this paper is organized as follows. The second section reviews the optimum tuning concept of TMDs and the studied methods in the literature. The third section briefly discusses the special attributes of NF ground motions and introduces the earthquakes that have been used in post tuning assessments. In the fourth section, the CBO algorithm, its pseudo-code as applied in the present study, and the optimization steps are expressed. In the fifth section, the optimum values of the TMD tuning parameters are calculated by considering the H_2 and H_∞ norm of roof displacement transfer function as the objective functions and compared with other researches. In the sixth section, the controlled structure performance is evaluated and compared to the closed-form expressions presented in the literature under NF and FF earthquakes. Finally, in the last section, the concluding remarks and the possible future research directions are outlined.

2 Optimum design of TMD

The main research area of TMD concerns its tuning i.e., optimizing the TMD mechanical parameters ξ_d (the damping ratio of the TMD) and f (the ratio of the damper frequency to the structural frequency) such that distinct response indices are minimized under different base or mass excitations. The control device conceived by Frahm did not have any damping, so the main concept of TMD modified with damping elements can be introduced with reference to a single-degree-of-freedom system (SDOF) displayed in Fig. 1a. The ratio of the TMD mass (m_d) to structural mass (M) represented with μ is an important design parameter usually preselected because of construction limitation. Although higher mass ratios are justifiable (Matta [6]), TMD mass is generally selected between 1 to 15 percent of the main mass, K and C are the stiffness and damping coefficient of the structure, k_d and c_d are the stiffness and damping coefficient of the damper. Moreover, the damper frequency (ω_d) and structural frequency (ω_s) are defined by Eq. (1) and Eq. (2), respectively as follows:

$$\omega_d = \sqrt{\frac{k_d}{m_d}} \tag{1}$$

$$\omega_s = \sqrt{\frac{K}{M}} \tag{2}$$

At the end of the past century, optimum values of these parameters were determined in several studies for multi-degree-of-freedom (MDOF) systems. A controlled MDOF is shown in Fig. 1(b) where i = 1, 2, …, N denotes the ith

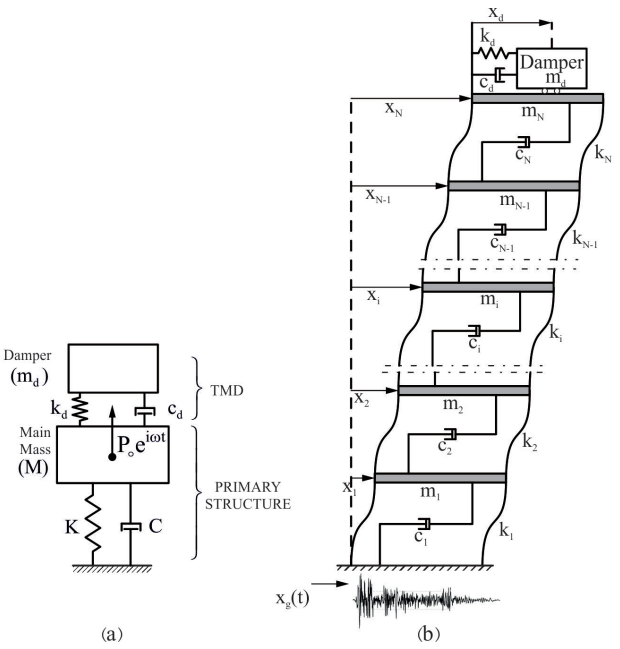

Fig. 1 Development of the TMD concept: (a) main concept of TMD under mass excitation (harmonic loading) (Warburton and Ayorinde, [12]), (b) *N* degree-of-freedom structure with a TMD under earthquake excitation (Sadek et al. [10])

degree of freedom of the main structure, while $N + 1$ is the degree of freedom of the attached TMD (Sadek et al. [10], Villaverde and Koyama [11]). Additionally, simple expressions were proposed for the optimum frequency ratio (f_{opt}) and damping ratio ($\xi_{d,opt}$) under FF seismic records (Sadek et al. [10]; Salvi et al. [9], Warburton and Ayorinde [12]) and NF seismic records (Matta [6]).

For example, based on the work of Brock in the frequency domain, Den Hartog [13] applied the famous fixed point method for the undamped main structure and proposed closed-form tuning *formulae* to compute the optimum frequency and damping ratios of TMDs under harmonic excitation of the main mass. The concept of fixed point method has been extended by Warburton and Ayorinde [12] for lightly damped main structures and more complex elastic bodies such as cylindrical shells under the random base and mass excitation. Additionally, the possibility and accuracy in idealizing MDOF main systems as a SDOF system are studied successfully.

Thompson [14] provided graphical solutions based on a frequency locus method for tuning TMD. For main structures with inherent damping conventional mathematical methods are difficult to be implemented. Therefore, usually numerical iterations are adopted for the optimum design of TMDs in damped structures. Tsai and Lin [15] suggested a numerical iteration searching technique to minimize the steady-state response of a damped main system under base excitation and found the optimum free parameters (i.e., frequency and damping ratios) of the TMD. Moreover, they used the curve-fitting method to propose closed-form formulae for the resulting optimum absorber parameters.

Another approach for selecting the optimum design parameters of TMDs is solving the eigenvalue problem and providing equal and large damping ratios in the first two complex modes of vibrations by using curve-fitting to numerically searched values and modifying the expression for MDOF systems (Sadek et al. [10], Villaverde and Koyama [11]). With the help of parametric studies, Rana and Soong [17] developed a simplified procedure for optimum tuning of TMDs, and they also studied the effect of detuning on the TMD performance. A Minimax optimization algorithm which takes advantage of the available *fminimax* function within MATLAB was proposed by Salvi and Rizzi [18], and the optimum free parameters of a TMD under seismic vibrations were calculated.

At TMD context, the first use of metaheuristic techniques was suggested by Hadi and Arfiadi [19]. They considered an H_2 performance index and employed a Genetic Algorithm (GA) to obtain the optimum values of TMD parameters under earthquake excitations. Desu et al. [20] employed a Nondominated Sorting Genetic Algorithm (NSGA) to control coupled lateral and torsional vibrations of asymmetric buildings with a coupled tuned mass damper. Leung et al. [21] applied Particle Swarm Optimization (PSO) algorithm to extract the optimum parameters (i.e. the mass and damping ratios of TMD and the tuning frequency) for a viscously damped SDOF system subject to non-stationary excitation considering the displacement or acceleration mean square response or their combination as the cost function.

Bekdaş and Nigdeli [22] applied the Harmony search (HS) for TMD parameters optimization under seismic excitations, and optimization criteria were selected the peak values of first story displacement and acceleration transfer function. In a subsequent paper, Bekdaş et al. [23] proposed a modified novel optimization approach employing the bat algorithm for a 10-story civil structure, and the outcomes are then compared with the analytical methods and other methods such as GA, PSO, and HS. Farshidianfar and Soheili [24] considered a 40-story frame building subjected to a given seismic record, with seismic analysis carried out in the time domain and TMD parameters optimized through an Ant Colony Optimization (ACO) method; however, the conclusions are yet under discussion

(Rahai et al. [25]). Kaveh et al. [26] hybridized Charged System Search (CSS) with HS for improving the exploitation to calculate optimum values of the TMD parameters under seismic excitations.

3 Earthquakes database and NF characteristics

NF earthquakes recorded within several kilometers of the fault rupture zone have different characteristics from their FF counterparts. In recent years, the response of the controlled SDOF and MDOF structures subjected to NF earthquakes has been investigated and affected from two distinct displacement patterns that depend on the rupture process and corresponding directivity effect (Bhagat et al. [27], Ke et al. [28], Vafaei and Eskandari [29]). Forward-directivity and fling-step are two special characteristics of NF earthquakes that can produce these motions. In a strike-slip fault rupture, the former occurs at fault-normal direction if the velocity of fault rupture propagation toward the site is close to the shear-wave velocity. Thus, at the beginning of the record, most of the seismic energy reaches the site within a short time in the form of a huge energy pulse. The latter occurs at fault-parallel direction of a strike-slip fault rupture as a result of tectonic movements and a permanent ground displacement accumulates at the site. Therefore, in the velocity and displacement time histories of earthquakes, both effects may result in large-amplitude, short duration, long-period pulses particularly important for the structural response of long-period structures (Kalkan and Kunnath [30], Matta [6]).

In this study, the structural responses are calculated for two sets of recorded NF ground motions possessing forward-directivity or fling-step features and are compared with the structural responses under a suite of FF accelerograms to address the influence of these three types of strong motion groups on the controlled structural performance. Each suite has 25 accelerograms and is represented in Tables 1 and 2 for FF and NF earthquakes, respectively (Bhagat et al. [27], Kalkan and Kunnath [30]).

Table 1 FF ground motions

No.	Year	Record	Station	Ref.	Comp.	PGA (g)
1	1992	Big Bear	Desert Hot Spr. (New Fire Stn.)	[32]	090	0.23
2	1994	Northridge	Laguna	[31]	90	0.22
3	1994	Northridge	Century CCC	[32]	090	0.26
4	1994	Northridge	Moorpark (Ventura Fire Stn.)	[32]	180	0.29
5	1987	Whittier-Narrows	Tarzana	[31]	90	0.54
6	1994	Northridge	Saturn Street School	[32]	S70E	0.43
7	2004	Parkfield	Parkfield	[31]	0	0.29
8	1952	Kern county	Taft	[31]	111	0.18
9	1971	San Fernando	Castaic, Old Ridge Route	[31]	291	0.27
10	1979	Imperial-Valley	Calexico	[31]	225	0.27
11	1994	Northridge	La-Habra	[31]	90	0.21
12	1994	Northridge	Lakewood	[31]	0	0.14
13	1994	Northridge	Ranchos-Palos	[31]	5	0.17
14	1994	Northridge	Montebello	[31]	206	0.18
15	1994	Northridge	Terminal Island Fire Stn. 111	[31]	330	0.19
16	1994	Northridge	Buena-Park	[31]	90	0.14
17	1994	Northridge	Santa FE	[31]	30	0.14
18	1994	Northridge	La-Puente	[31]	105	0.13
19	1994	Northridge	Baldwin-Park	[31]	270	0.12
20	1992	Landers	Baker	[31]	50	0.11
21	1952	Kern county	SantaBarbara Courthouse	[31]	132	0.13
22	1986	N. Palm Springs	Temecula	[31]	0	0.12
23	1986	N. Palm Springs	Anza Tule Canyon	[31]	270	0.11
24	1989	Loma Prieta	Presidio	[31]	0	0.10
25	1987	Whittier-Narrows	Glendora	[31]	170	0.11

Table 2 NF ground motions

NF ground motions (flinf-step)							NF ground motions (forward-directivity)						
No.	Year	Record	Station	Ref.	Comp.	PGA (g)	No.	Year	Record	Station	Ref.	Comp.	PGA (g)
1	1999	Chi-Chi	TCU052	[34]	EW	0.35	1	1979	Imperial-Valley	Brawley Airport	[31]	225	0.16
2	1999	Chi-Chi	TCU052	[34]	NS	0.44	2	1979	Imperial-Valley	El Centro Array #3	[31]	230	0.22
3	1999	Chi-Chi	TCU068	[34]	EW	0.50	3	1979	Imperial-Valley	El Centro Diff. Array	[31]	270	0.35
4	1999	Chi-Chi	TCU068	[34]	NS	0.36	4	1979	Imperial-Valley	El Centro Imp. Co. Cent.	[31]	092	0.23
5	1999	Chi-Chi	TCU074	[34]	EW	0.59	5	1979	Imperial-Valley	Holtville Post Office	[31]	315	0.22
6	1999	Chi-Chi	TCU074	[34]	NS	0.37	6	1999	Kocaeli	Duzce	[31]	180	0.31
7	1999	Chi-Chi	TCU084	[34]	EW	0.98	7	1989	Loma Prieta	Gilroy STA #2	[31]	000	0.37
8	1999	Chi-Chi	TCU129	[34]	EW	0.98	8	1989	Loma Prieta	Gilroy STA #3	[31]	090	0.37
9	1999	Kocaeli	Yarimca	[33]	EW	0.23	9	1994	Northridge	Rinaldi Rec. Stn.	[32]	S49W	0.84
10	1999	Kocaeli	Izmit	[33]	EW	0.23	10	1984	Morgan Hill	Coyote Lake Dam	[32]	285	1.16
11	1999	Kocaeli	Sakarya	[33]	EW	0.41	11	1994	Northridge	Slymar Converter Sta East	[31]	018	0.83
12	1999	Chi-Chi	TCU102	[34]	EW	0.29	12	1979	Imperial-Valley	El Centro Array #7	[32]	S50W	0.46
13	1999	Chi-Chi	TCU089	[34]	EW	0.34	13	1994	Northridge	Jensen Filt. Plant	[31]	022	0.42
14	1999	Chi-Chi	TCU049	[34]	EW	0.27	14	1994	Northridge	Newhall LA Fire Stn.	[31]	090	0.58
15	1999	Chi-Chi	TCU067	[34]	EW	0.48	15	1994	Northridge	Sylmar Olive View Hospital	[31]	360	0.84
16	1999	Chi-Chi	TCU075	[34]	EW	0.32	16	1984	Morgan Hill	Anderson Dam	[32]	340	0.29
17	1999	Chi-Chi	TCU076	[34]	EW	0.33	17	1987	Superstition Hills	Parachute Test Site	[31]	315	0.45
18	1999	Chi-Chi	TCU072	[34]	NS	0.36	18	1994	Northridge	Newhall Pico Canyon	[31]	046	0.45
19	1999	Chi-Chi	TCU072	[34]	EW	0.46	19	1989	Loma Prieta	Corralitos	[31]	000	0.64
20	1999	Chi-Chi	TCU065	[34]	EW	0.76	20	2004	Parkfield	Cholame 1E	[35]	FN	0.47
21	1999	Chi-Chi	TCU079	[34]	EW	0.57	21	2004	Parkfield	Cholame 5W (Sta 5)	[35]	FN	0.21
22	1999	Chi-Chi	TCU078	[34]	EW	0.43	22	2004	Parkfield	Fault Zone 1	[35]	FN	0.50
23	1999	Chi-Chi	TCU082	[34]	EW	0.22	23	2004	Parkfield	Gold Hill 1W	[35]	FN	0.13
24	1999	Chi-Chi	TCU128	[34]	EW	0.14	24	1992	Cape Mendocino	Petrolia, General Store	[31]	090	0.66
25	1999	Chi-Chi	TCU071	[34]	NS	0.63	25	1992	Erzincan	Erzincan	[31]	EW	0.50

4 Optimization procedure

H_∞ optimization is the first proposed optimization criterion. The objective is to minimize the maximum amplitude of the magnification factor (called H_∞ norm) of the system. The H_2 optimization criterion is to reduce the total vibration energy of the system at all frequencies. In this optimization criterion, the area (called H_2 norm) under the frequency response curve of the system is minimized (Asami et al. [36]). In this paper, it is attempted that with a simple procedure and somehow different from previous researches, optimization simply and quickly is performed, and then design graphs are generated for optimum design of TMD. Therefore, the norms of the transfer function are preferred as the objective function. Thus, the optimum parameters are independent of external excitation frequency content, and the control methods are robust. However, to make the optimization more efficient and to consider the importance of the first mode in the final response, an equivalent SDOF structure is defined based on the first mode characteristics, and the TMD optimum parameters are obtained for this equivalent structure.

General steps for the calculation of the TMD optimum parameters for this equivalent structure are:

1. Frequency analysis is performed and natural frequencies and modal shapes are realized.
2. Dynamical properties of the first mode (mass, stiffness, and damping) are determined, and an equivalent SDOF structure is constructed.
3. CBO algorithm is employed to find the TMD optimum parameters as a function of mass ratio (μ) and different inherent structural damping ratio ξ_s In this procedure, minimizing the H_∞ and H_2 norm (Eq. (3) and Eq. (4), respectively) of the equivalent structure roof displacement are selected as the objective function separately.

$$\mathbf{H}_{\infty} = \sup_{\omega} \bar{\sigma}\left(\mathbf{H}\right), \tag{3}$$

$$\mathbf{H}_{2} = \sqrt{\text{trace}\left[\frac{1}{2\pi}\int_{-\infty}^{+\infty} \mathbf{H}^{*}\mathbf{H} d\omega\right]}, \tag{4}$$

where $\bar{\sigma}$ and $\sup_{\omega}$ represent the greatest singular value of the transfer function matrix and the smallest upper bound of $\bar{\sigma}$ for all frequencies, respectively. Here, **H** is the transfer function that relates the input (base excitation) to the output (roof displacement) of the system. Additionally, the frequency and damping ratios of the TMD are selected as the design variables. In Matlab vector notation, the ranges of these variables are considered as follows:

$$f = [0.55{:}0.01{:}1.2],\ \xi_{d} = [0{:}0.005{:}0.5]. \tag{5}$$

4. The optimum design of TMD (i.e., optimum frequency and damping ratios) as a function of mass ratio and inherent damping ratio is computed. Design graphs are developed in which optimum parameters are calculated based on the proposed method and compared with the closed-form *formulae* presented in the literature.

4.1 Colliding Bodies Optimization algorithm

Having a simple formulation, the CBO is one of the metaheuristic algorithms proposed by Kaveh and Mahdavi [37]. The CBO needs no internal parameters tuning and this is an interesting feature of this algorithm. The CBO pseudo-code for a minimization problem is as follow (Kaveh [38]):

Set initial position for 2N-CBs randomly
Repeat
For each CB the objective function is calculated
The mass of CBs is assigned proportioned inversely to its fitness value
The CBs are lined up in ascending order based on their mass
The organized CBs are divided into two parts
The CBs in the second part move toward their relevant CBs in the first part.
CBs are colliding with each other and their velocity after the collision is evaluated
The new positions of CBs are calculated in terms of their after collision velocities
Until the termination criteria are fulfilled.
Output: founded best solution

In this study, the number of CBs and steps that are used in the optimization process are 20 and 30, respectively. Some other application of CBO can be found in Kaveh and Ilchi Ghazaan [39], Kaveh [40], Kaveh et al. [41] and Kaveh and Sabeti [42].

Other metaheuristics can also be used in place of CBO. Examples of such metaheuristic can be found in Kaveh [40] and code for such algorithms can be found in Kaveh and Bakhshpoori [43].

5 Numerical example

In this section, a benchmark 10-story shear building is assessed (Sadek et al. [10]). The structural properties are reported in Table 3. In this building, a TMD on the top of the structure is added to control the structural responses under external excitations.

Optimum free parameters at different values of mass ratio (μ) and four different inherent structural damping ratios (ξ_s = 0, 2, 5, and 10 pct.) are calculated, and optimum values of the free parameters are plotted as a function of μ in Figs. 2 and 3. In these figures, closed-form *formulae* suggested by Sadek et al. [10], Matta [6], and Salvi and Rizzi [44] derived for MDOF structures are plotted for comparison. In Table 4, a brief of stated closed-form *formulae* is tabulated. The Matta *formula* is the only TMD tuning *formula* under near-fault records calculated for ξ_s = 2 pct., and the values of its coefficient, pj, can be found in the original paper [6].

As can be seen, the present calibration procedures have the same general pattern with those proposed in the literature; however, the obtained trend of optimum frequency and damping ratios are in close agreement with Sadek et al. [10], and Salvi and Rizzi [44] estimation, respectively. It should be noted that Sadek et al. [10] revealed the detuning effect of Villaverde [16] *formula* when the mass ratio is increased. They displayed that if the frequency ratio is set equal to one, by increasing the mass ratio, optimum parameters determined based on Villaverde [16] method are not optimum.

It should be noted that Matta [6] has presented the TMD optimum damping *formulae* for structures with 2 pct. inherent damping ratio. Since for all other tuning methods and different inherent damping ratios, the TMD optimum damping ratio has an almost similar curve, also in the Matta method for different damping ratios, the TMD optimum damping ratio curve considered unchanged. As can be seen in Fig. 2, for all considered methods, Matta [6] and Sadek et al. [10] methods obtain the lowest and highest TMD optimum damping estimates respectively, so their poor and enhanced performance in the next section can be justified by their TMD optimum damping estimations.

Table 3 Structural parameters of the 10-story building (Sadek et al. [10]).

Story	Mass ($\times 10^3$ kg)	Stiffness ($\times 10^6$ N/m)	Story	Mass ($\times 10^3$ kg)	Stiffness ($\times 10^6$ N/m)	Mode Number	Freq. (Hz)	Mode Number	Freq. (Hz)
1	179	62.47	**6**	134	46.79	**1**	0.50	**6**	4.29
2	170	59.26	**7**	125	43.67	**2**	1.33	**7**	4.84
3	161	56.14	**8**	116	40.55	**3**	2.15	**8**	5.27
4	152	53.02	**9**	107	37.43	**4**	2.93	**9**	5.59
5	143	49.91	**10**	98	34.31	**5**	3.65	**10**	5.79

Table 4 Closed-form expressions for tuning free parameters of TMD

Methods	Year	$f_{opt} = \frac{\omega_{d,opt}}{\omega_s}$	$\xi_{d,opt} = \frac{c_{d,opt}}{2m_d\omega_{d,opt}}$
Sadek et al. [10]	1997	$\frac{1}{1+\phi\mu}[1-\xi_s\sqrt{\frac{\phi\mu}{1+\phi\mu}}]$	$\phi(\frac{\xi_s}{1+\mu}+\sqrt{\frac{\mu}{1+\mu}})$
Matta (Matta [6]	2013	$\frac{\sqrt{(1-\mu/2)}}{1+\mu}$ / $1+p_1\sqrt{\mu}+\mu^3[p_2-p_3/(1+p_4\mu^5)]$	$\frac{p_5\mu^4-p_6\mu^3+p_7\mu^2-p_8\mu}{\mu^3-p_9\mu^2+p_{10}\mu-p_{11}}$
Salvi and Rizzi (Salvi and Rizzi [44])	2016	$1-\sqrt{3\mu}(\frac{2}{3}\sqrt{\mu}+\frac{3}{2}\zeta_s)$	$\frac{1}{2}\sqrt{\propto}$

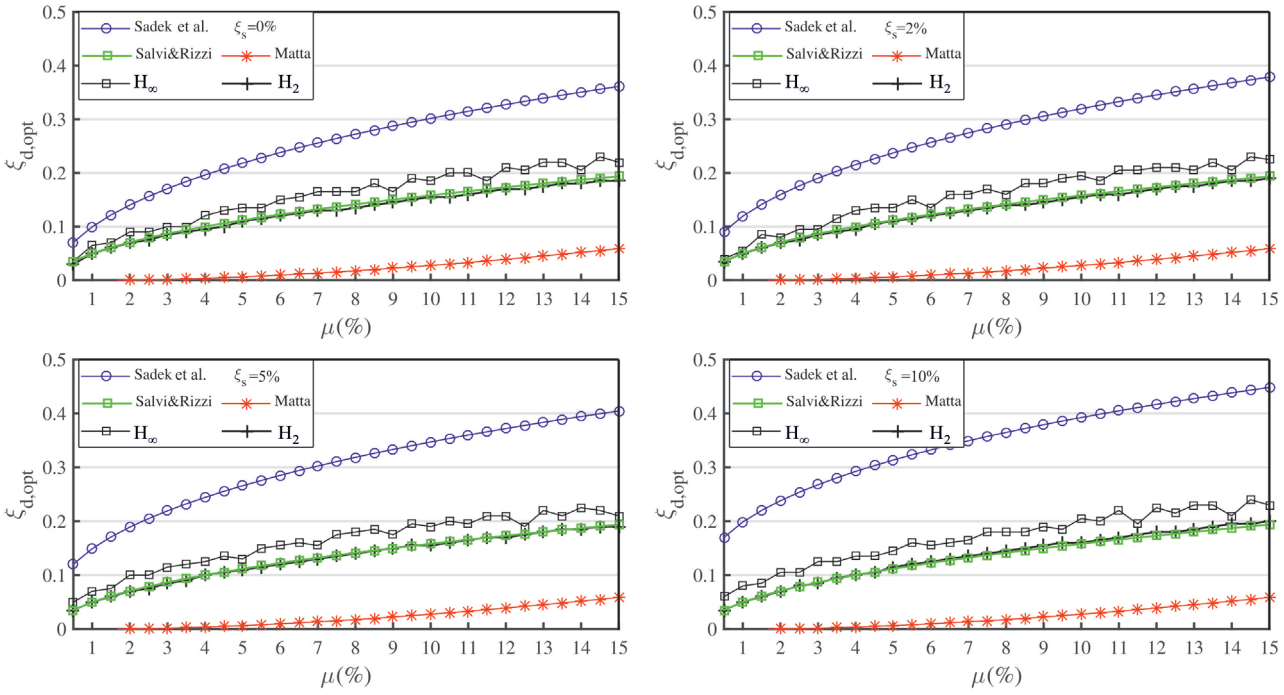

Fig. 2 Optimum damping ratio (ξ_d-opt) as a function of mass ratio (μ) and four different inherent damping ratios

6 Performance assessment of optimally designed TMD under different earthquakes

In this section, the performance of the controlled 10-story shear building is carried out in terms of the attained design graphs from the previous section under three suites of 25 natural earthquake excitations (i.e., NF earthquakes with forward-directivity, fling-step, and FF earthquakes). In Figs. 4–11, the designed TMD functionality is evaluated and discussed for a structure with 0 pct. inherent structural damping. In suppressing the structural vibrations, displacement and absolute acceleration are two important criteria when structural safety or human comfort is of primary importance, respectively. Therefore, the peak and RMS of roof displacement and acceleration are selected as performance indices. Afterward, the same evaluation and discussion are summarized in Figs. 12–19 for structures

with 5 pct. inherent structural damping ratio. In all plotted figures and both assumed inherent damping ratios, since the H_∞ method outperforms the H_2 approach, the diagrams of H_∞ technique have been included in all figures. Thus, all implemented methods are compared with the H_∞ algorithm allowing also the identification of the pros and cons of the discussed procedures. Different tuning algorithms i.e., Matta [6], H_2, Sadek et al. [10] and Salvi and Rizzi [44] (based on displacement and acceleration criteria, shown in green and black colors, respectively) are compared to the H_∞ method (shown in red, blue, and orange colors for NF earthquakes with forward-directivity, fling-step, and FF earthquakes, respectively). In each graph, the abscissa shows the mass ratio in the range of 0.5 to 15 pct., and for each mass ratio, the mean of controlled to uncontrolled response with its one standard deviation confidence interval is plotted as a solid line and shaded area respectively over 25 records in the corresponding database.

6.1 Displacement criterion for structure with 0 pct. inherent damping ratio

To provide a better comparison between performance and efficiency of different approaches, the controlled to uncontrolled maximum and RMS of roof displacement are calculated and plotted in Figs. 4–6. These figures show the performance of controlled structure at different mass ratios and for structure with 0 pct. inherent damping ratio under the NF groups of records with forward-directivity, fling-step, and FF group of records, respectively.

For considering uncertainty in the natural ground motions and quantifying the resulted uncertainty in the structural response, results are illustrated in terms of mean and mean plus/minus one standard deviation of controlled to uncontrolled structural responses subjected to 25 earthquakes in each set. Each figure has two rows, and each graph in the first and second rows compares the controlled to uncontrolled maximum and RMS of roof displacement respectively for different tuning methods. Generally, all techniques except the Matta method indicate a similar trend, and the structural response reduces considerably under all ensembles of records with increasing the TMD mass ratio. In contrast, the Matta method does not follow the common trend, and as the mass ratio increases, its performance curve initially deviates from the other methods which leads to the highest discrepancy from other curves and the TMD worst performance at 0.5-5 pct. mass ratios. However, after an overshoot especially apparent subjected to ground motions with fling-step, it consistently and quickly gets close to the other curves for higher mass ratios. Additionally, as was predicted by the analysis in Section 4, the Matta method is also inferior regarding variance reduction, and as a consequence has an unreliable improved performance.

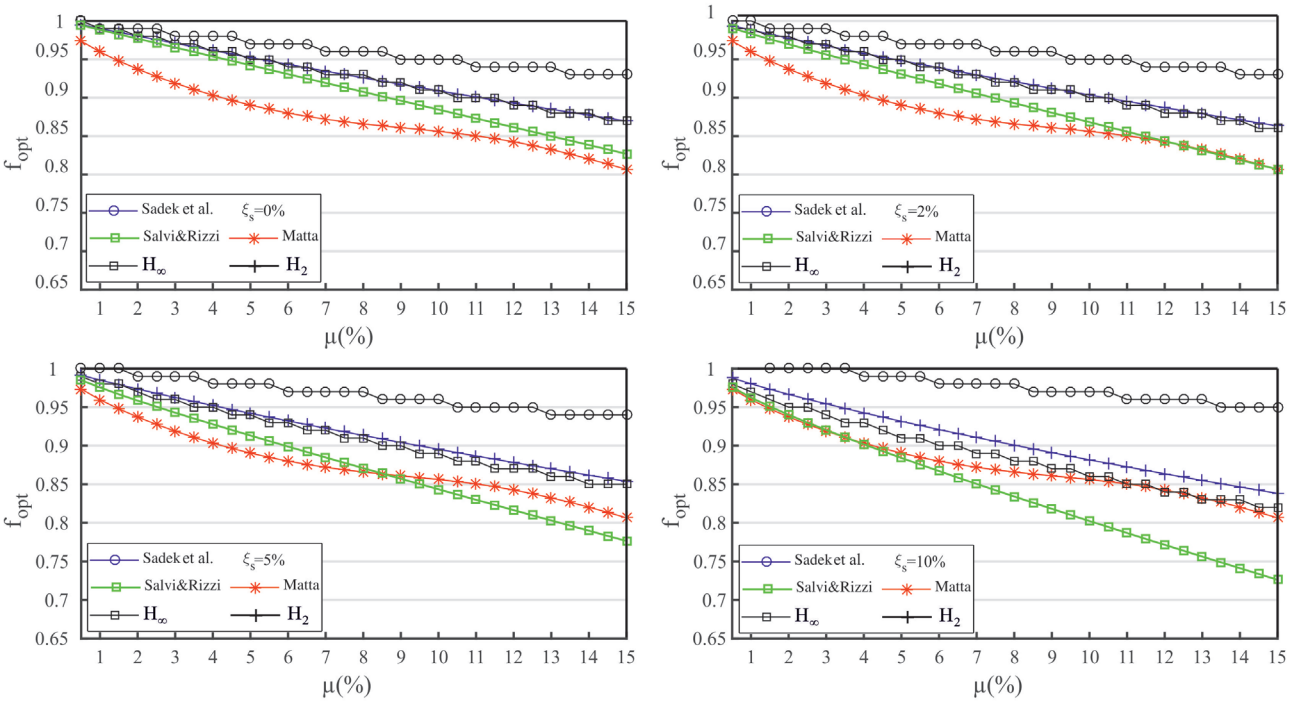

Fig. 3 Optimum frequency ratio (f_{opt}) as a function of mass ratio (μ) and four different inherent damping ratios

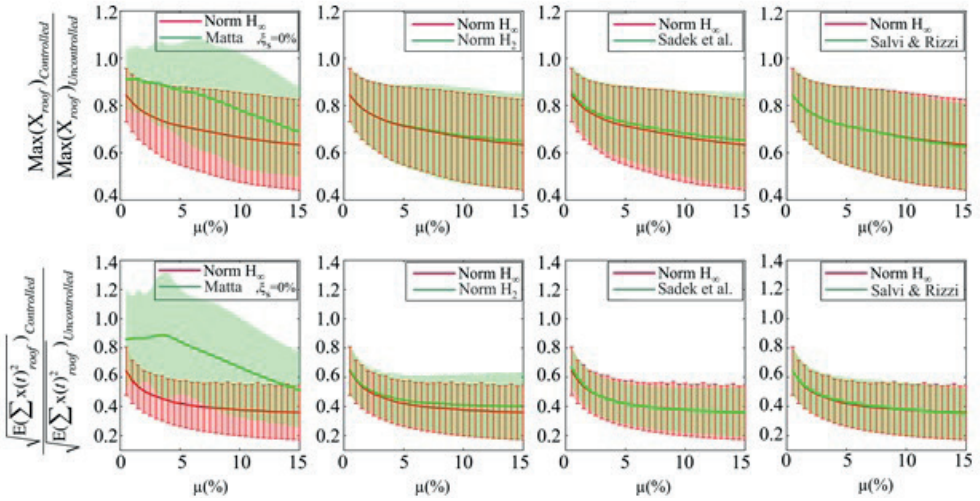

Fig. 4 Normalized controlled to uncontrolled maximum and RMS of the structural roof displacement under earthquakes with forward-directivity (0 pct. inherent damping ratio)

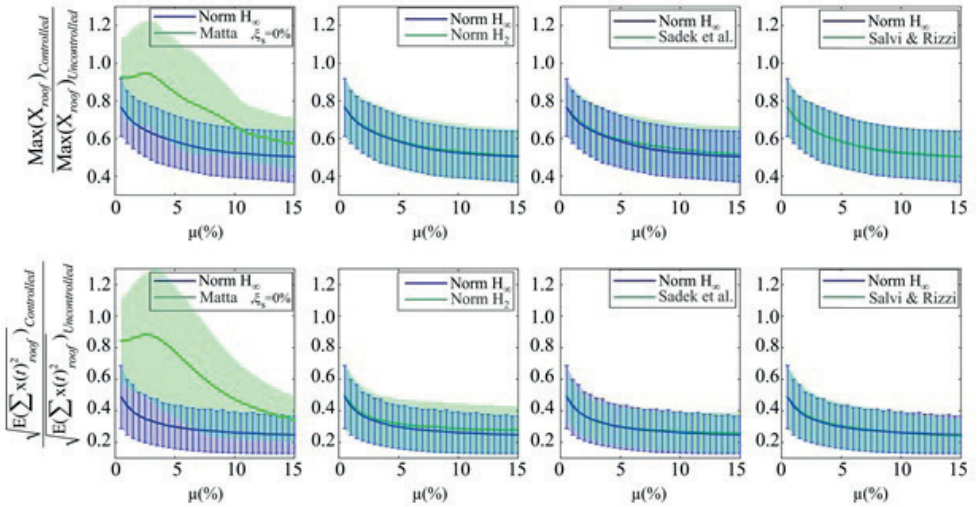

Fig. 5 Normalized controlled to uncontrolled maximum and RMS of the structural roof displacement under earthquakes with fling-step (0 pct. inherent damping ratio)

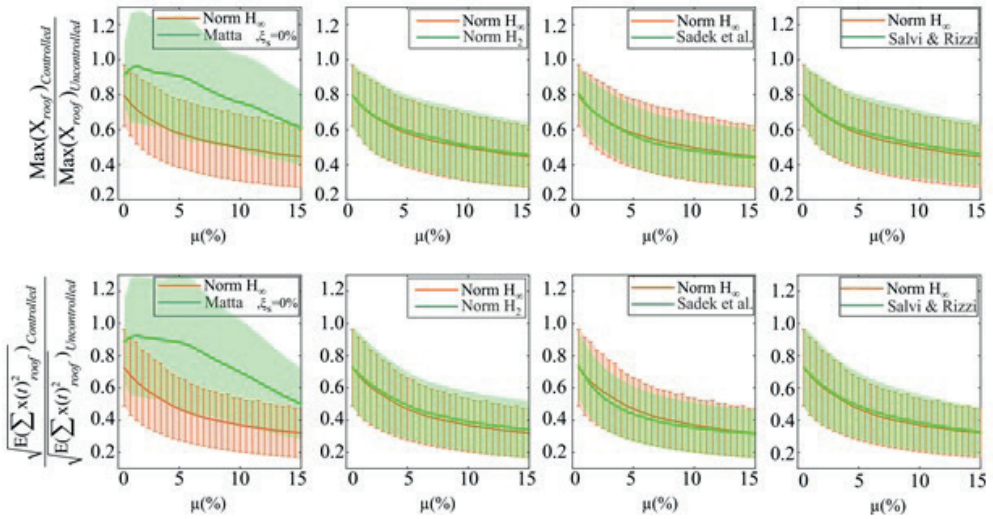

Fig. 6 Normalized controlled to uncontrolled maximum and RMS of the structural roof displacement under FF earthquakes (0 pct. inherent damping ratio)

Since optimum designed TMD based on the Matta method [6] has the smallest optimum damping between other methods and similar tuning frequency, this result supports a hypothesis that the main cause for damping input energy is the TMD damping. Thus, for the Matta method, the performance of TMD can be increased, and the uncertainty of the Matta method can be reduced by increasing the TMD damping ratio, which leads to smaller variance and significantly enhances the performance.

As far as the control method robustness is concerned, (i.e., controlled to uncontrolled response < 1), all adapted methods are robust, nevertheless the Matta tuning *formula* has the worst performance under all studied criteria, and its corresponding shaded area at some mass ratios gets values substantially greater than one. Between the remaining methods, although they have very similar performance, in almost all cases, the H_∞ has slightly superior performance. However, under FF earthquakes the Sadek et al. [10] and under NF earthquakes the Salvi and Rizzi method [44] have slightly better performance.

Because of the very similar performance of the H_2, Sadek et al. [10], Salvi and Rizzi [44] and the H_∞ approach, to facilitate the understanding of the TMD performance under three different earthquake sets, the displacement responses of TMD designed with H_∞ procedure are compared in Fig. 7.

The TMD performance shows that the NF ground motions with forward-directivity impose higher maximum roof displacement, nevertheless the TMD under NF earthquakes with fling-step characteristic exhibit the best performance in the case of RMS of roof displacement.

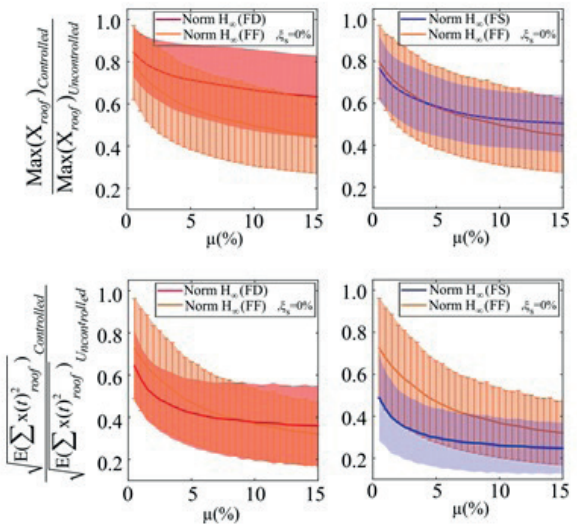

Fig. 7 Normalized controlled to uncontrolled Maximum and RMS of the structural roof displacement under FF and NF earthquakes with forward-directivity or fling-step characteristics (0 pct. inherent damping ratio)

The rate of increasing TMD performance diminishes as the mass ratio increases for NF earthquakes in contrast to FF counterparts and reaches a steady-state (at about 10 pct. mass ratio). The standard deviation in NF earthquakes with forward-directivity grows considerably as the mass ratio increases, but it remains almost constant under two other suites of seismic records.

6.2 Acceleration criterion for structure with 0 pct. inherent damping ratio

In Figs. 8–10, at different mass ratios and 0 pct. inherent damping ratio, the controlled to uncontrolled maximum and RMS of roof acceleration are calculated and plotted under different earthquake sets.

For acceleration criteria, similar patterns to displacement criteria can be seen i.e., for all methods, generally, the performance of TMD enhances as the mass ratio increases. However, the rate of increasing the TMD performance in terms of acceleration criteria is much higher than the results obtained for the displacement criteria. However, the three methods with similar performance for displacement criteria have much distinct performance based on acceleration criteria. Additionally, one of the pronounced differences between acceleration and displacement criteria is the reduction of the confidence interval in the former criteria, and as a result, acceleration response has smaller uncertainty. In all of the investigated methods and under all earthquake sets, the ratios of controlled to uncontrolled structural responses with one standard deviation are smaller than one although the Matta method is the only exception. Accordingly, all considered methods are robust excluding the Matta method which although its mean is always less than one, its mean plus one standard deviation gets values greater than one especially in small mass ratios. Thus, it is not robust under earthquake uncertainty.

Under three record groups, the best performance belongs to Sadek et al. [10], then H_∞, Salvi and Rizzi [44], and H_2 methods, and the Matta method shows the worst performance with a considerable difference anticipated with its small TMD optimum damping ratio values. Consequently, this result ascertains the weighty contribution of TMD optimum damping ratio in the acceleration reduction effect of considered methods.

The acceleration response of the controlled structure with the H_∞ method subjected to all record sets is compared in Fig. 11. The TMD under FF ground motions has the worst performance omitting the case of maximum roof acceleration which TMD has the worst performance

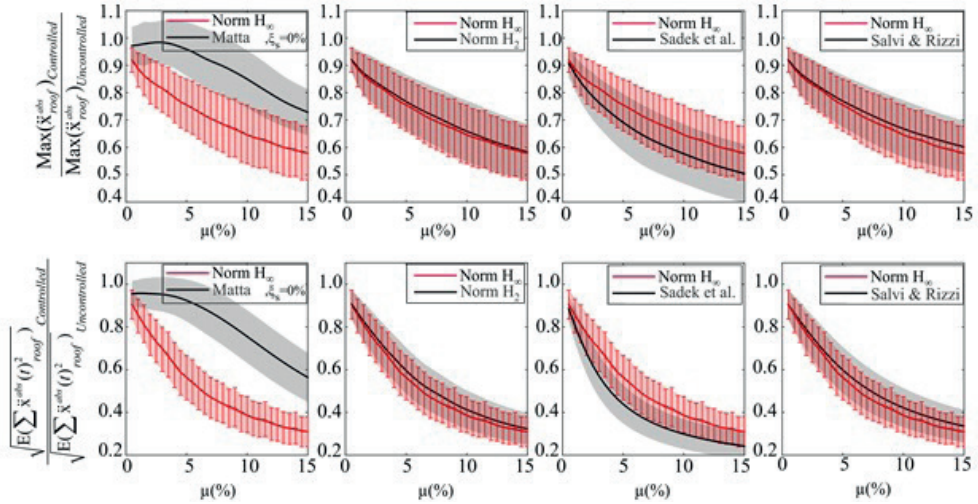

Fig. 8 Normalized controlled to uncontrolled maximum and RMS of the structural roof acceleration under earthquakes with forward-directivity (0 pct. inherent damping ratio)

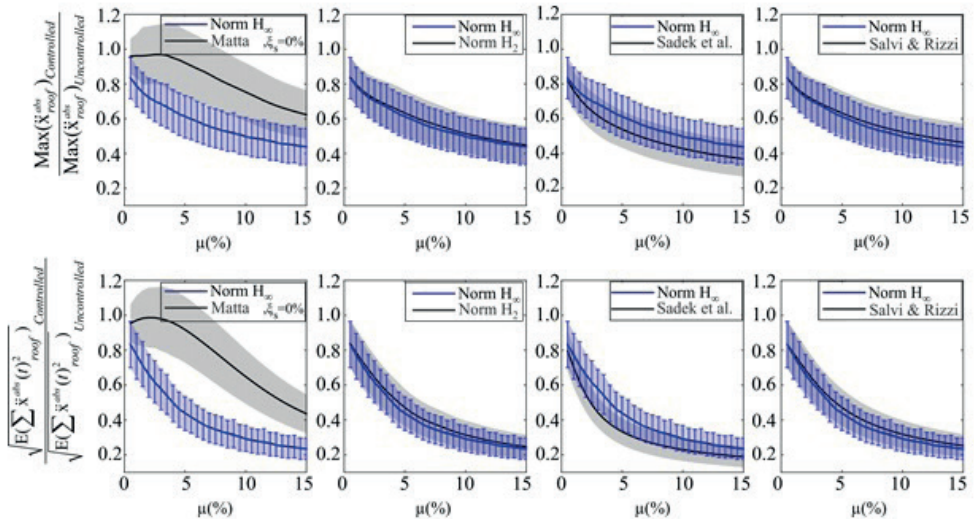

Fig. 9 Normalized controlled to uncontrolled maximum and RMS of the structural roof acceleration under earthquakes with fling-step (0 pct. inherent damping ratio)

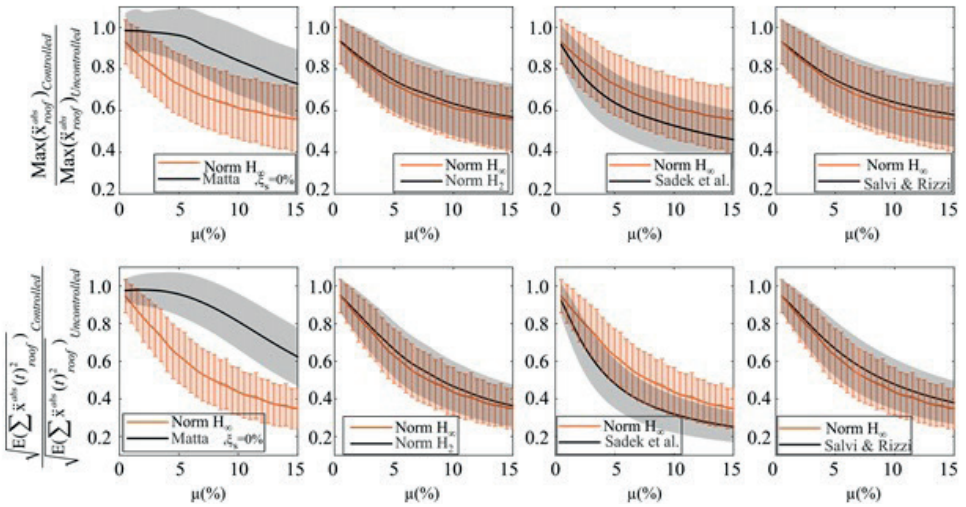

Fig. 10 Normalized controlled to uncontrolled maximum and RMS of the structural roof acceleration under FF earthquakes (0 pct. inherent damping ratio)

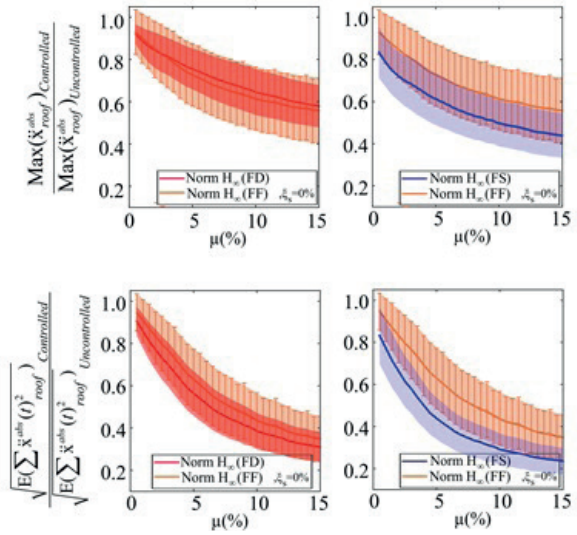

Fig. 11 Normalized controlled to uncontrolled Maximum and RMS of the structural roof acceleration under FF and NF earthquakes with forward-directivity or fling-step characteristics (0 pct. inherent damping ratio)

under NF earthquakes with forward-directivity; however, the largest standard deviation in all plots belongs to TMD performance under FF earthquakes.

For the RMS criterion, the confidence interval remains almost consistent under all record suites. However, it will expand as the mass ratio increases especially for maximum roof acceleration criterion under FF and NF earthquakes with forward-directivity.

Overall, both results of displacement and acceleration criteria suggest that in practice, Sadek et al. [10] method reduces the mean and variance of both criteria, which leads to significantly improved performance and less uncertainty between all considered methods because of its largest optimum damping ratio.

6.3 Displacement criterion for structure with 5 pct. inherent damping ratio

Real structures have small inherent structural damping ratio usually assumed 5 pct. of critical damping. Therefore, to further investigate the effect of inherent structural damping on the TMD performance, the previous figures are derived for the 10-story shear building with 5 pct. inherent damping ratio and are plotted in Figs. 12–19. The same trend is observed for the performance of the damped structure although there are some apparent differences with undamped structural responses. The TMD is demonstrated to be more effective on the structure with a lower damping level, from a comparison of Figs. 4–11 with Figs. 12–19.

Based on all proposed methods, the performance of designed TMD has decreased considerably for a structure with 5 pct. inherent structural damping as in Figs. 12–14. According to the displacement criteria and in almost all cases, the H_∞ method outperforms other methods although for larger mass ratios the Salvi and Rizzi method [44] has a faintly improved performance, and the same results can be noted under all records.

By increasing the mass ratio, although the performance gets enhanced in many cases, the confidence interval upper bound gets very close to one. However, in almost all mass ratios, the considered methods are still robust excluding the Matta method which its confidence interval upper bound crosses the uncontrolled threshold (i.e., controlled to uncontrolled response = 1). Furthermore, the confidence interval spread by increasing the mass ratio in all cases which indicates the sensitivity of the designed TMD to earthquake uncertainty.

Although the confidence interval remains consistent in almost all cases for structure with 0 pct. inherent damping ratio, for 5 pct. inherent damping ratio, the confidence interval expands as the mass ratio increases in almost all considered criteria. Hence, the reliability of the estimated performance decreases. The H_∞ performance is very similar to Salvi and Rizzi technique for structure with 5 pct. inherent damping ratio which has the best performance, and its difference from other methods has increased especially in the case of the mean (solid line); however, the least confidence interval belongs to the Sadek et al. method [10]. The proposed methods (Salvi and Rizzi [44], Sadek et al. [10], H_2, and H_∞) are robust since their performance criterion never gets values larger than one. However, the Matta method is not robust and in most cases, its performance passes one. As a result, the application of the Matta approach is discouraged for all investigated mass ratios.

6.4 Acceleration criterion for structure with 5 pct. inherent damping ratio

In Figs. 16–19, the TMD performance is investigated according to the roof acceleration criteria and for structure with 5 pct. damping ratio, and the general pattern is identical to the undamped structure.

In the case of roof acceleration criteria based on either mean or confidence interval, the maximum TMD performance can be achieved by the Sadek et al. method [10] disregarding the small mass ratios in which the H_∞ method has the best performance. However, the difference between the TMD performance designed with the H_∞ and Sadek et al. methods is decreased considerably for structures with 5 pct. inherent damping ratio especially under NF earthquakes.

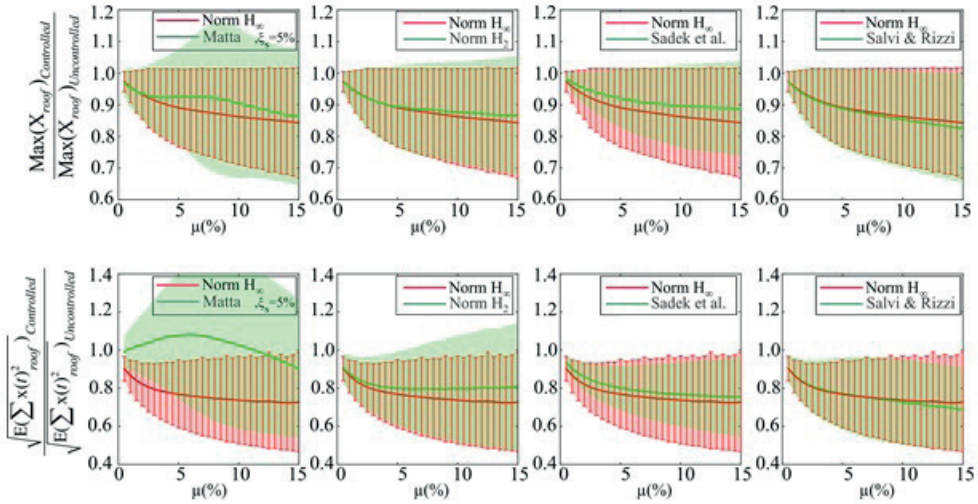

Fig. 12 Normalized controlled to uncontrolled maximum and RMS of the structural roof displacement under earthquakes with forward-directivity (5 pct. inherent damping ratio)

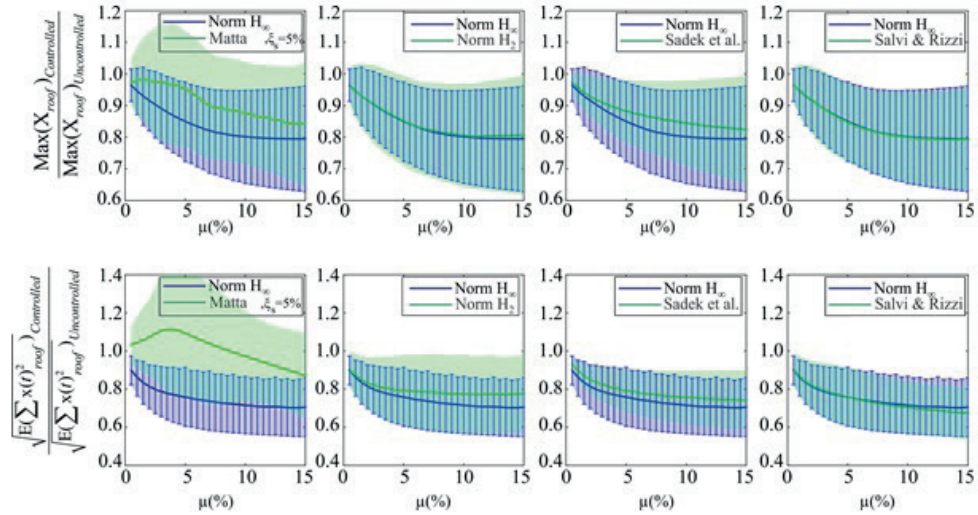

Fig. 13 Normalized controlled to uncontrolled maximum and RMS of the structural roof displacement under earthquakes with fling-step (5 pct. inherent damping ratio)

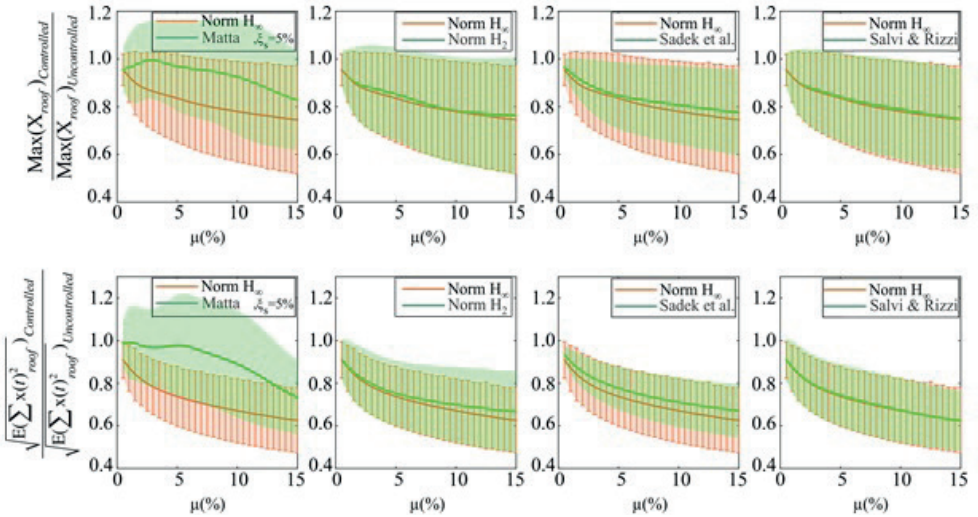

Fig. 14 Normalized controlled to uncontrolled maximum and RMS of the structural roof displacement under FF earthquakes (5 pct. inherent damping ratio)

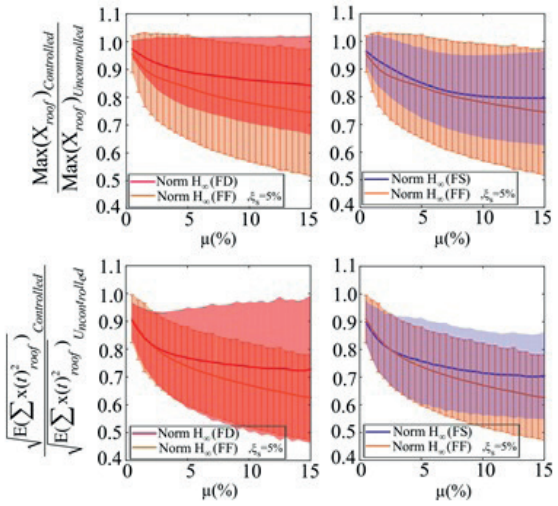

Fig. 15 Normalized controlled to uncontrolled maximum and RMS of the structural roof displacement under FF and NF earthquakes with forward-directivity or fling-step characteristics (5 pct. inherent damping ratio)

In Fig. 19, the efficiency of designed TMD with H_∞ method has been inspected under three distinct record sets for acceleration criteria. The general trends are identical to structure with 0 pct. damping although by raising the mass ratio, the rate of growing the TMD efficiency suppresses considerably. Furthermore, similar to undamped structures the TMD has the best performance under earthquakes with fling-step and the worst performance under the FF earthquakes.

7 Conclusions

This paper contrasts two proposed methods for optimum design of a TMD added to the roof of an MDOF structure with regards to the minimization of the H_2 and H_∞ of the roof displacement transfer function of an equivalent SDOF structure. Furthermore, the performance of designed TMD under NF earthquakes with forward-directivity and

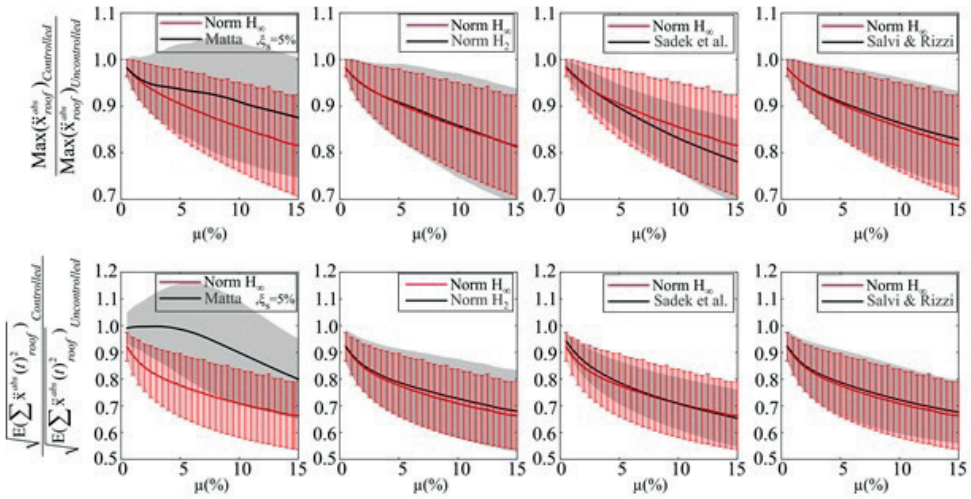

Fig. 16 Normalized controlled to uncontrolled maximum and RMS of the structural roof acceleration under earthquakes with forward-directivity (5 pct. inherent damping ratio)

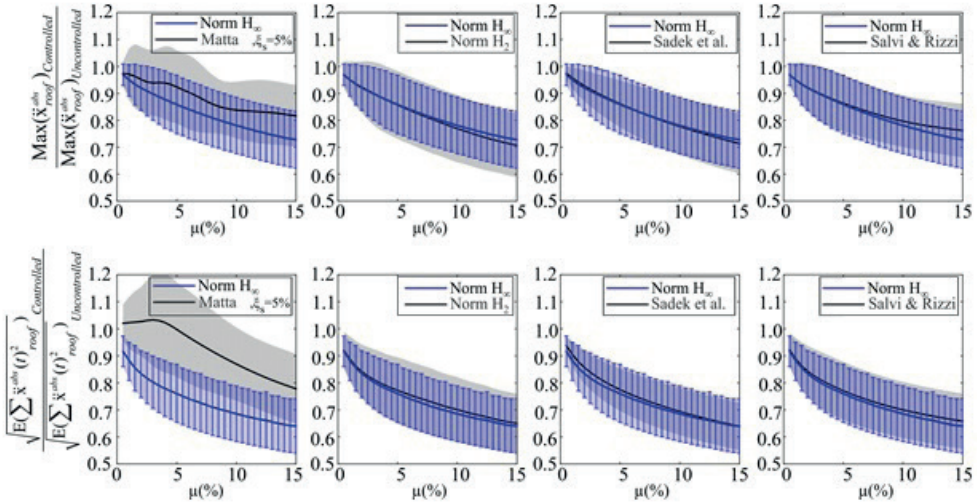

Fig. 17 Normalized controlled to uncontrolled maximum and RMS of the structural roof acceleration under earthquakes with fling-step (5 pct. inherent damping ratio)

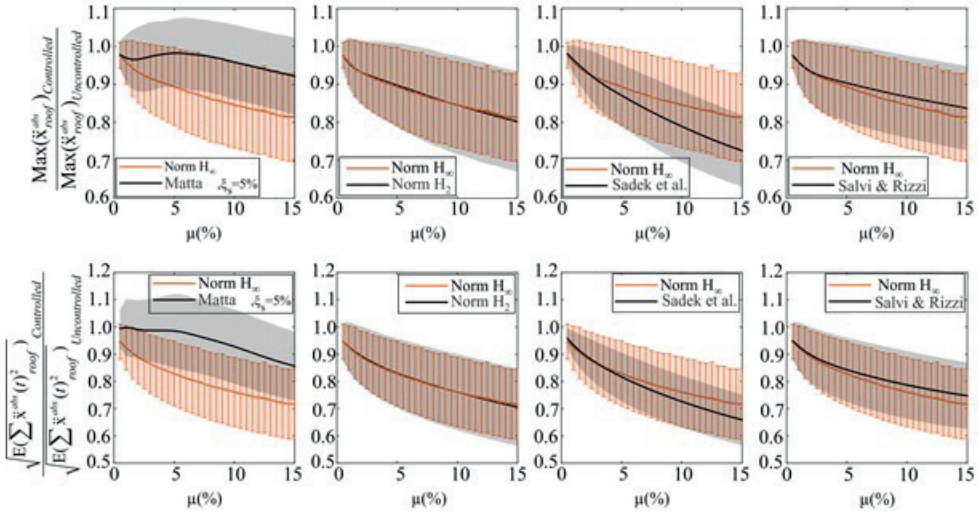

Fig. 18 Normalized controlled to uncontrolled maximum and RMS of the structural roof acceleration under FF earthquakes (5 pct. inherent damping ratio)

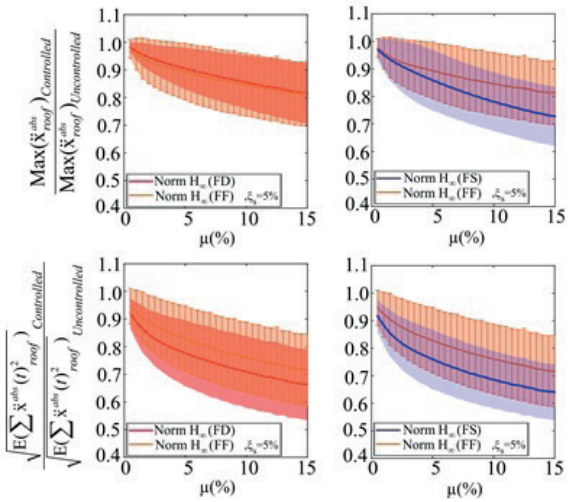

Fig. 19 Normalized controlled to uncontrolled maximum and RMS of the structural roof acceleration under FF and NF earthquakes with forward-directivity or fling-step characteristics (0 pct. inherent damping ratio)

fling-step characteristics and FF earthquakes are fully assessed. For a 10-story shear building, the TMD optimum parameters as a function of μ andare derived depending on the proposed methods and represented in design charts. Then, three distinct sets of earthquake excitations, which each set has 25 benchmark earthquakes, are applied to assess the performance of controlled structures based on four performance indices (i.e., peak and RMS of roof displacements and peak and RMS of roof accelerations). These indices are calculated for controlled structure with the proposed framework and other proposed formulae in the literature, and the outcomes are compared in probability context i.e., the mean with its one standard deviation confidence interval of the TMD performance under each set is plotted and compared. The results demonstrate similar performance for the H_2 and H_∞; however, the H_∞ method has marginally improved performance in comparison to the H_2 and other considered methods in most adopted cases. The H_∞ in parallel with the Salvi and Rizzi method [44] find the TMD optimum parameters especially for displacement criteria in such a way that in most cases dominate the other proposed formulae in mitigating the structural displacement. Though, for acceleration criteria, the best performance belongs to the Sadek et al. method [10]. Furthermore, with the concept of robust control, these approaches reduce the structural response under all three different suites of earthquake vibrations. Three characteristics of the proposed procedures are their simple implementation, robustness, and less computational cost. Finally, the performance of designed TMDs under the NF and FF earthquakes is compared which shows higher performance under the FF earthquakes concerning displacement criteria and the NF earthquakes in the case of acceleration criteria, especially for damped structures.

It should be tadded that the behavior of the shear-building is assumed as linear and the results are not valid when nonlinearity (both geometrical and material) is introduced into the equations. In addition, considering soil-structure interaction, the possibility to control the structure using a nonlinear TMD that can adjust its parameters passively based on the performance indices requires further investigation. Finally, the current study does not include the uncertainties in the structural parameters, and a mathematical model that can exactly reflect these uncertainties should be established.

Conflict of interest

Kaveh and co-authors have no conflict of interest.

References

[1] Elias, S., Matsagar, V. "Research developments in vibration control of structures using passive tuned mass dampers", Annual Reviews in Control, 44, pp. 129–156, 2017. https://doi.org/10.1016/j.arcontrol.2017.09.015

[2] Gutierrez Soto, M., Adeli, H. "Tuned Mass Dampers", Archives of Computational Methods in Engineering, 20, pp. 419–431, 2013. https://doi.org/10.1007/s11831-013-9091-7

[3] Lu, X., Zhang, Q., Weng, D., Zhou, Z., Wang, S., Mahin, S. A., Ding, S., Qian, F. "Improving performance of a super tall building using a new eddy-current tuned mass damper", Structural Control and Health Monitoring, 24(3), Article number: e1882, 2017. https://doi.org/10.1002/stc.1882

[4] Sun, J. Q., Jolly, M. R., Norris, M. A. "Passive, Adaptive and Active Tuned Vibration Absorbers - A survey", Journal of Mechanical Design, 117(B), pp. 234–242, 1995. https://doi.org/10.1115/1.2836462

[5] Lin, C.-C., Chen, C.-L., Wang, J.-F. "Vibration Control of Structures with Initially Accelerated Passive Tuned Mass Dampers under Near-Fault Earthquake Excitation", Computer-Aided Civil and Infrastructure Engineering, 25(1), pp. 69–75, 2010. https://doi.org/10.1111/j.1467-8667.2009.00607.x

[6] Matta, E. "Effectiveness of Tuned Mass Dampers against Ground Motion Pulses", Journal of Structural Engineering, 139(2), pp. 188–198, 2013. https://doi.org/10.1061/(ASCE)ST.1943-541X.0000629

[7] Domizio, M., Ambrosini, D., Curadelli, O. "Performance of tuned mass damper against structural collapse due to near fault earthquakes", Journal of Sound and Vibration, 336, pp. 32–45, 2015. https://doi.org/10.1016/j.jsv.2014.10.007

[8] Salvi, J., Rizzi, E., Rustighi, E., Ferguson, N. S. "On the optimization of a hybrid tuned mass damper for impulse loading", Smart Materials and Structures, 24(8), Article number: 085010, 2015. https://doi.org/10.1088/0964-1726/24/8/085010

[9] Salvi, J., Rizzi, E., Rustighi, E., Ferguson, N. S. "Optimum Tuning of Passive Tuned Mass Dampers for the Mitigation of Pulse-Like Responses", Journal of Vibration and Acoustics, 140(6), Article number: 061014, 2018. https://doi.org/10.1115/1.4040475

[10] Sadek, F., Mohraz, B., Taylor, A. W., Chung, R. M. "A method of estimating the parameters of tuned mass dampers for seismic applications", Earthquake Engineering and Structural Dynamics, 26(6), pp. 617–635, 1998. https://doi.org/10.1002/(SICI)1096-9845(199706)26:6<617::AID-EQE664>3.0.CO;2-Z

[11] Villaverde, R., Koyama, L. A. "Damped resonant appendages to increase inherent damping in buildings", Earthquake Engineering and Structural Dynamics, 22(6), pp. 491–507, 1993. https://doi.org/10.1002/eqe.4290220603

[12] Warburton, G. B., Ayorinde, E. O. "Optimum absorber parameters for simple systems", Earthquake Engineering and Structural Dynamics, 8(3), 197–217, 1980. https://doi.org/10.1002/eqe.4290080302

[13] Den Hartog, J. P. "Mechanical Vibrations", 4th ed., Dover Publications, Mineola, NY, USA, 1956.

[14] Thompson, A. G. "Optimum tuning and damping of a dynamic vibration absorber applied to a force excited and damped primary system", Journal of Sound and Vibration, 77(3), pp. 403–415, 1981. https://doi.org/10.1016/S0022-460X(81)80176-9

[15] Tsai, H.-C., Lin, G.-C. "Optimum tuned-mass dampers for minimizing steady-state response of support-excited and damped systems", Earthquake Engineering and Structural Dynamics, 22(11), pp. 957–973, 1993. https://doi.org/10.1002/eqe.4290221104

[16] Villaverde, R. "Reduction seismic response with heavily-damped vibration absorbers", Earthquake Engineering and Structural Dynamic, 13(1), pp. 33–42, 1985. https://doi.org/10.1002/eqe.4290130105

[17] Rana, R., Soong, T. T. "Parametric study and simplified design of tuned mass dampers", Engineering Structures, 20(3), pp. 193–204, 1998. https://doi.org/10.1016/S0141-0296(97)00078-3

[18] Salvi, J., Rizzi, E. "Optimum tuning of Tuned Mass Dampers for frame structures under earthquake excitation", Structural Control and Health Monitoring, 22(4), 707–725, 2015. https://doi.org/10.1002/stc.1710

[19] Hadi, M. N. S., Arfiadi, Y. "Optimum Design of Absorber for MDOF Structures", Journal of Structural Engineering, 124(11), pp. 1272–1280, 1998. https://doi.org/10.1061/(ASCE)0733-9445(1998)124:11(1272)

[20] Desu, N. B., Deb, S. K., Dutta, A. "Coupled tuned mass dampers for control of coupled vibrations in asymmetric buildings", Structural Control and Health Monitoring, 13(5), pp. 897–916, 2006. https://doi.org/10.1002/stc.64

[21] Leung, A. Y. T., Zhang, H., Cheng, C. C., Lee, Y. Y. "Particle swarm optimization of TMD by non-stationary base excitation during earthquake", Earthquake Engineering and Structural Dynamics, 37(9), pp. 1223–1246, 2008. https://doi.org/10.1002/eqe.811

[22] Bekdaş, G., Nigdeli, S. M. "Estimating optimum parameters of tuned mass dampers using harmony search", Engineering Structures, 33(9), pp. 2716–2723, 2011. https://doi.org/10.1016/j.engstruct.2011.05.024

[23] Bekdaş, G., Nigdeli, S. M., Yang, X.-S. "A novel bat algorithm based optimum tuning of mass dampers for improving the seismic safety of structures", Engineering Structures, 159, pp. 89–98, 2018. https://doi.org/10.1016/j.engstruct.2017.12.037

[24] Farshidianfar, A., Soheili, S. "Ant colony optimization of tuned mass dampers for earthquake oscillations of high-rise structures including soil–structure interaction", Soil Dynamics and Earthquake Engineering, 51, pp. 14–22, 2013. https://doi.org/10.1016/j.soildyn.2013.04.002

[25] Rahai, A. R., Saberi, H., Saberi, H. "A Discussion of the paper: "Ant colony optimization of tuned mass dampers for earthquake oscillations of high-rise structures including soil–structure interaction" [Soil Dyn. Earthq. Eng. 51 (2013) 14–22]", Soil Dynamics and Earthquake Engineering, 102, pp. 263–265, 2017. https://doi.org/10.1016/j.soildyn.2016.03.011

[26] Kaveh, A., Mohammadi, S., Khadem Hosseini, O., Keyhani, A., Kalatjari, V. R. "Optimum parameters of tuned mass dampers for seismic application using charged system search", Iranian Journal of Science and Technology, Transactions of Civil Engineering, 39(C1), pp. 21–40, 2015.
https://doi.org/10.22099/ijstc.2015.2739

[27] Bhagat, S., Wijeyewickrema, A. C., Subedi, N. "Influence of Near-Fault Ground Motions with Fling-Step and Forward-Directivity Characteristics on Seismic Response of Base-Isolated Buildings", Journal of Earthquake Engineering, 2018.
https://doi.org/10.1080/13632469.2018.1520759

[28] Ke, K., Zhao, Q., Yam, M. C. H., Ke, S. "Energy factors of trilinear SDOF systems representing damage-control buildings with energy dissipation fuses subjected to near-fault earthquakes", Soil Dynamics and Earthquake Engineering, 107, pp. 20–34, 2018.
https://doi.org/10.1016/j.soildyn.2017.12.023

[29] Vafaei, D., Eskandari, R. "Seismic performance of steel mega braced frames equipped with shape-memory alloy braces under near-fault earthquakes", Structural Design of Tall and Special Buildings, 25(1), pp. 3–21, 2016.
https://doi.org/10.1002/tal.1225

[30] Kalkan, E., Kunnath, S. K. "Effects of Fling Step and Forward Directivity on Seismic Response of Buildings", Earthquake Spectra, 22(2), pp. 367–390, 2006.
https://doi.org/10.1193/1.2192560

[31] University of Berkeley "Pacific Earthquake Engineering Research Center (PEER)" [online] Available at: https://ngawest2.berkeley.edu/

[32] Organizations for Strong Motion Observation Systems (COSMOS) "Center for Engineering Stron Motion Data" [online] Available at: https://strongmotioncenter.org/

[33] Republic of Turkey Prime Ministry "Disaster & Emergency Management Authority Presidential of Earthquake Department" [online] Available at: https://deprem.afad.gov.tr

[34] Central Weather Bureau Seismological Center "Disastrous shocks" [online] Available at: https://scweb.cwb.gov.tw/en-us/page/disaster

[35] California Department of Conservation "The California Strong Motion Instrumentation Program (CSMIP)" [online] Available at: https://www.conservation.ca.gov/cgs/smip

[36] Asami, T., Nishihara, O., Baz, A. M. "Analytical solutions to H∞ and H2 optimization of dynamic vibration absorbers attached to damped linear systems", Journal of Vibration and Acoustics, 124(2), pp. 284–295, 2002.
https://doi.org/10.1115/1.1456458

[37] Kaveh, A., Mahdavi, V. R. "Colliding bodies optimization: A novel meta-heuristic method", Computers and Structures, 139, pp. 18–27, 2014.
https://doi.org/10.1016/j.compstruc.2014.04.005

[38] Kaveh, A. "Advances in Metaheuristic Algorithms for Optimal Design of Structures", 2nd ed., Springer, Cham, Switzerland, 2017.
https://doi.org/10.1007/978-3-319-05549-7

[39] Kaveh, A., Ilchi Ghazaan, M. "A comparative study of CBO and ECBO for optimal design of skeletal structures", Computers and Structures, 153, pp. 137–147, 2015.
https://doi.org/10.1016/j.compstruc.2015.02.028

[40] Kaveh, A. "Applications of Metaheuristic Optimization Algorithms in Civil Engineering", Springer, Cham, Switzerland, 2017.
https://doi.org/10.1007/978-3-319-48012-1

[41] Kaveh, A., Mahdavi, V. R., Kamalinejad, M. "Optimal Design of the Monopole Structures using CBO and ECBO Algorithms", Periodica Polytechnica Civil Engineering, 61(1), pp. 110–116, 2017.
https://doi.org/10.3311/PPci.8546

[42] Kaveh, A., Sabeti, S. "Optimal Design of Jacket Supporting Structures for Offshore Wind Turbines Using CBO and ECBO Algorithms", Periodica Polytechnica Civil Engineering, 62(3), pp. 545–554, 2018.
https://doi.org/10.3311/PPci.11651

[43] Kaveh, A., Bakhshpoori, T. "Metaheuristics: Outlines, MATLAB Codes and Examples", Springer, Cham, Switzerland, 2019.
https://doi.org/10.1007/978-3-030-04067-3

[44] Salvi, J., Rizzi, E. "Closed-form optimum tuning formulas for passive Tuned Mass Dampers under benchmark excitations", Smart Structures and Systems, 17(2), pp. 231–256, 2016.
https://doi.org/10.12989/sss.2016.17.2.231